Desalination and Water Treatment
www.deswater.com

doi: 10.5004/dwt.2019.24776

171 (2019) 281–293
December

Production of adsorbent from activated carbon of palm oil shells coated by Fe_3O_4 particle to remove crystal violet in water

Buhani[a,*], Suharso[a,*], Fitria Luziana[a], Mita Rilyanti[a], Sumadi[b]

[a]*Department of Chemistry, Faculty of Mathematic and Natural Sciences, University of Lampung, Indonesia, Jl. Soemantri Brojonegoro No. 1 Bandar Lampung, Indonesia, 35145, Tel. +62721704625; Fax: +62721702767; emails: buhani_s@yahoo.co.id (Buhani), suharso_s@yahoo.com (Suharso)*
[b]*Department of Electrical Engineering, Faculty of Engineering, University of Lampung, Indonesia, Jl. Soemantri Brojonegoro No. 1 Bandar Lampung, Indonesia, 35145*

Received 8 April 2019; Accepted 5 August 2019

ABSTRACT

This study focused on making environmentally friendly activated carbon (AC) derived from palm oil shells producing a palm-based powdered activated carbon (PPAC) coated with Fe_3O_4 particles (PPAC-Fe_3O_4) as an adsorbent to adsorb crystal violet (CV) dyes in water. Activation of carbon from oil palm shells was carried out chemically using a H_3PO_4 solution of 10%. The characterization results of PPAC-Fe_3O_4 adsorbent using X-ray diffraction, nitrogen adsorption–desorption isotherms, and scanning electron microscopy-energy dispersive-X ray (SEM-EDX) compared with PPAC show that the coating process of Fe_3O_4 particle on PPAC has been carried out successfully to produce the adsorbent of PPAC-Fe_3O_4. Adsorption of CV dyes on PPAC and PPAC-Fe_3O_4 was optimum at pH 10 with an adsorbent dose of 2.5 g L^{-1}, and contact time of 90 min. The CV dye adsorption kinetics model on PPAC and PPAC-Fe_3O_4 tends to follow the pseudo-second-order kinetic model with the rate constants (k_2) for PPAC and PPAC-Fe_3O_4 of 0.059 and 0.088 g mg^{-1} min^{-1}, respectively. In addition, the adsorption isotherm model of CV dyes on PPAC and PPAC-Fe_3O_4 tends to follow the Freundlich adsorption isotherm with K_F values of 1.066 and 2.852 (mg g^{-1}) (L mg^{-1})$^{1/n}$, respectively. This indicates that the CV dye adsorption process occurs on heterogeneous surfaces with multilayer that occur through the pores of activated carbon and the magnetic properties of PPAC-Fe_3O_4 have increased the number of adsorbed CV dye.

Keywords: Activated carbon; Activated carbon-Fe_3O_4; Adsorption; Crystal violet; Palm oil shells

1. Introduction

Water pollution is still one of the problems that need to be considered because it has a serious impact on water sources and the balance of environmental ecosystems. Water pollution has its origin from industrial, agricultural and household waste, which is caused by the presence of chemicals such as dyes, phenols, detergents, pesticides, insecticides, heavy metals, and other pollutants released into the environment [1–4]. One industry that produces a lot of waste that pollutes waters is the textile industry. Dyes from industrial water are observable pollutants that are complicated to control because of their complicated molecular characteristic and synthetic source. The dyes detached into the surrounding may cause critical effects on exposed organisms because of the dye toxicity [5,6].

Crystal violet (CV) is a triphenylmethane dye with the molecular formula $C_{25}N_3H_{30}Cl$ widely used as a dermatological agent in various commercial textile processes [7]. Crystal violet is carcinogenic and it is grouped as obstinate

* Corresponding authors.

molecule, because it is non-biodegradable, is difficult metabolized by microbes, and can stand in various environments [8]. Crystal violet dyes are found as one of the agents that cause poisoning in aquatic ecosystems that lead problems for living things [9,10]. Therefore, to reduce the danger that can be caused from the residual disposal of CV dyes, the reduction of these dyes in industrial waste needs to be done, especially in the treatment of waste before the spread occurs to the environment.

Various methods have been widely used to reduce dyes in wastes such as oxidation [11,12], coagulation and flocculation [13], adsorption [14,15], ion exchange [16], biological treatment [17], and magnetic separation method [18]. From the various methods mentioned, the adsorption method is the most widely used method because it has high efficiency [15,19]. In addition, the adsorption also has other advantages such as cheap process, simple method, safe for environment, and no toxic side effects [20–22].

Various adsorbents such as activated carbons [23], clays [24,25], and carbon nanotubes [26] were successfully used to remove dyes from aqueous solution. The most widely used adsorbent for the adsorption process in industrial wastewater treatment systems is activated carbon due to its large specific surface area [27–29].

Regarding the use of activated carbon, the market demand for AC is increasing. Therefore, efforts need to be made to produce AC from agro-industrial waste, such as waste originating from oil palm shells. One of the most commonly used AC application is as an adsorbent in processing chemical wastes. The use of AC as an adsorbent is carried out by considering the policy of applying the zero waste concept, namely utilizing agro-industrial waste to reduce other industrial wastes such as toxic chemicals [30–32]. But along with the increase in the number and types of waste found in the environment, it is also necessary to improve the quality of activated carbon which has a more specific character to be effectively used as an adsorbent.

Activated carbon has advantages as an adsorbent in many aspects, but has limitations in the separation of the remaining AC by-products and also the limitations of regeneration for repeated use [22]. In addition, the filtration and centrifugation processes in the adsorption process often time consuming [15]. The barrier of filters and the lapse of adsorbents can happen in filtration process. Centrifugation is not an economic process. The application of magnetic separation method proposes an alternative method to complete these matters [33–35].

Therefore it is necessary to improve the AC quality; one of the methods is to provide magnetic properties to the AC through superparamagnetic (Fe_3O_4) particle coating techniques. The magnetic properties of activated carbon can separate the adsorbate quickly and the adsorption process takes place at room temperature [36]. The material coating technique with magnetite particles is an environmental friendly technique, because it does not form products that contain contamination such as suspended solids, besides it accelerates the process of separating metals from solution because the adsorbent is magnetic [37–40]. In addition, coating AC with Fe_3O_4 will produce a stable AC in acidic conditions [41].

In this study, it was carried out production of an adsorbent from palm-based powdered activated carbon (PPAC), which was coated with Fe_3O_4 particles (PPAC-Fe_3O_4) to adsorb crystal violet (CV) dyes. By using this technique, it was obtained PPAC-Fe_3O_4 which has a large adsorption rate and capacity for the CV dyes in solution and can separate target compounds quickly, effectively and does not cause by-products that are harmful to the environment. This is one of the solutions to utilize the palm oil shells as industrial agro waste into the material that has an economic value and can be used as an adsorbent in the treatment of a toxic chemical waste to reduce an environmental pollution.

2. Materials and methods

2.1. Materials

The materials used in this study were palm oil shells originating from palm oil processing waste in Lampung Province, Indonesia. Crystal violet, sodium hydroxide, potassium nitrate, and $FeSO_4{\cdot}7H_2O$ were purchased from European Pharmacopoeia, (France) with AR grade. To obtain a stock solution with a concentration of 1 g L^{-1}, as much as 1 g of the CV dye (Basic violet 3) dye was dissolved in water to a volume of 1 L. For this study, the concentrations of CV dye at range of 10–300 mg L^{-1} were made from the stock solutions. The absorbance of the CV dye was displayed in the range of 585–598 nm (UV-Vis spectrophotometer, Cary 100, Agilent, USA). All the experiments in this study used double distilled water.

2.2. Preparation of activated carbon

Before the carbonation process was carried out, the palm shells were washed first with water to remove the waste, then dried in the sun. Dried palm oil shells were inserted into the furnace to be carbonized, and they were activated by flowing water vapor into the furnace. The carbonization process was carried out at a temperature of 600°C for 60 min. The carbon was smoothed and sieved with a 200 micron sieve. Refined carbon was chemically activated using a 10% H_3PO_4 solution according to the procedures carried out [7,42] to produce activated carbon powder from the palm oil shells (PPAC).

2.3. Synthesis of activated carbon-Fe_3O_4

Synthesis of PPAC-Fe_3O_4 was done by dissolving 27 g of $FeSO_4{\cdot}7H_2O$ into 200 mL of distilled water and adding 50 g of PPAC. Then the suspension was heated at 80°C for 2 h, added drop by drop 50 mL of a base solution made from a mixture of 2.25 g of KNO_3 and 15 g of NaOH while stirring constantly with a magnetic stirrer. Then the resulting suspension was sonicated at 80°C for 1 h and stored overnight. The results of the suspension were filtered and washed with distilled water to neutral pH and dried in an oven at 60°C [36].

2.4. Adsorbent characterization

The PPAC and PPA-Fe_3O_4 adsorbents were characterized by X-ray diffraction (XRD; Shimadzu 6000, Japan) to determine the level of material crystallinity. Investigation of specific surface area and pore volumes was analyzed using

a surface area analyzer (Quantachrome TouchWin v1.0, Florida, U.S.A.). The surface morphology and constituent elements were identified by SEM-EDX (Zeiss MA10, Germany).

2.5. Zero point charge (pH_{pzc}) measurement

The zero charge (pH_{pzc}) of the PPAC and PPAC-Fe_3O_4 was determined using 0.1 M of NaCl aqueous solutions at pH 3–10. These pH values were fixed with either a 0.1 N of HCl or 0.1 N of NaOH aqueous solution. These solutions (10 mL of each) were brought into contact with 0.05 g of sample and the system was stirred for 48 h. The supernatant was then decanted and its pH was measured. The pH_{pzc} value was obtained from a plot of pH of the initial solution against pH of the supernatant.

2.6. Adsorption experiments

Adsorption process of the CV dye on PPAC and PPAC--Fe_3O_4 adsorbents was carried out using the batch method through the stirring process using a shaker (Stuart-reciprocating shaker, SSL2, Cole-Parmer, Illinois, U.S.A.). In the experiments with the batch method, a CV dye solution with an initial concentration of 10–300 mg L^{-1} was used. For each experiment, a certain amount of PPAC or PPAC-Fe_3O_4 and 20 mL of CV dye solution were moved in a flask, and stirred in a temperature-controlled shaker with a constant speed of 200 rpm for a contact time of 0–120 min and various pHs of 3–12. At destined time intervals, 5 mL of dispersion was taken and isolated quickly by an adscititious magnet to gather adsorbent. For PPAC adsorbents, the adsorbate separation from the adsorbent was carried out using centrifugation and filtration. The supernatant containing residual CV dye was analyzed at 590 nm by UV-Vis spectrophotometer (Cary 100, Agilent, USA). The concentration of CV dye was measured from a calibration curve of absorbance against concentration of CV dye. All measurements were carried out in triplicate per experiment. The adsorption studies were performed with various factors of the pH, dosage adsorbent, contact time, and initial concentration. In order to control the pH of the CV dye solution, 0.1 mol L^{-1} of HCl or NaOH solution was added with ignored volume.

The amount of CV dye adsorbed per mass unit of adsorbent and the percentage of adsorbed CV dye were determined using Eqs. (1) and (2), respectively:

$$q = \frac{(C_0 - C_e)v}{w} \quad (1)$$

$$\text{Removal}(\%) = \frac{(C_0 - C_e)}{C_0} \times 100 \quad (2)$$

where C_0 and C_e (mg L^{-1}) are the CV dye concentration before and after the adsorption process, w is the amount of adsorbent (g), and v is the volume of solution (L), q is the amount of CV dye adsorbed per mass unit (mg g^{-1}).

2.7. Reusability adsorbent

Reuse of the PPAC-Fe_3O_4 adsorbent to adsorb the CV dye was studied by carrying out five repetitions of CV dye adsorption process. The adsorption was carried out by interacting 250 mg of adsorbent with CV dye solution of 100 mg L^{-1} at pH of 10, contact time of 90 min, and temperature of 27°C. The release of CV dye adsorbed on the adsorbent was eluted using 0.05 M HCl solution. Regeneration of the adsorbent was rinsed with distilled water to neutral pH and dried at 60°C for 24 h, then reused for repeated adsorption.

3. Results and discussion

3.1. Synthesis and characterization of adsorbent

Synthesis of PPAC material was performed by activating carbon from oil palm shells chemically using 10% H_3PO_4 solution followed by coating Fe_3O_4 particles to produce PPAC-Fe_3O_4. The two adsorbents were characterized including identification of functional groups with IR spectrometers, crystalline levels with XRD, surface area, and pore volume with the BET method, as well as surface morphology and constituent elements of material with SEM-EDX.

Fig. 1 displays the XRD pattern of Fe_3O_4, PPAC, and PPAC-Fe_3O_4. In the figure, it can be seen that the presence of a wide asymmetrical peak at 2θ from 25°–45° which indicates a typical form of carbon amorph [36,43,44]. The XRD pattern on PPAC-Fe_3O_4 shows a change in the reduction of the amorphous carbon phase to the crystalline phase which is characterized by the presence of a diffraction peak at 30.05°; 35.55°; 43.37°; 57.43°; and 62.91° derived from Fe_3O_4 nanocrystal [15,41] as found in the Fe_3O_4 diffraction pattern. This shows that coating of Fe_3O_4 particles in PPAC has occurred.

Based on the IUPAC classification, the N_2 adsorption–desorption isotherms of PPAC and PPAC-Fe_3O_4 (Fig. 2a) showed a tendency to follow the pattern of the adsorption–desorption isotherms of the combined type from the adsorption isotherms of type I and IV. The adsorption isotherm pattern of the type I occurs in low P/P_0 regions, it is seen that the form of isotherm tends to be horizontal. The type I adsorption isotherm patterns only form one layer of adsorbate and only occur in the chemisorption

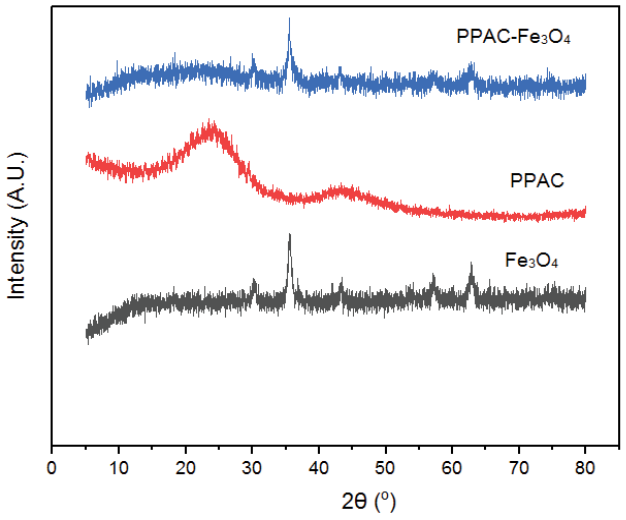

Fig. 1. XRD patterns of (a) Fe_3O_4, (b) PPAC, and (c) PPAC-Fe_3O_4.

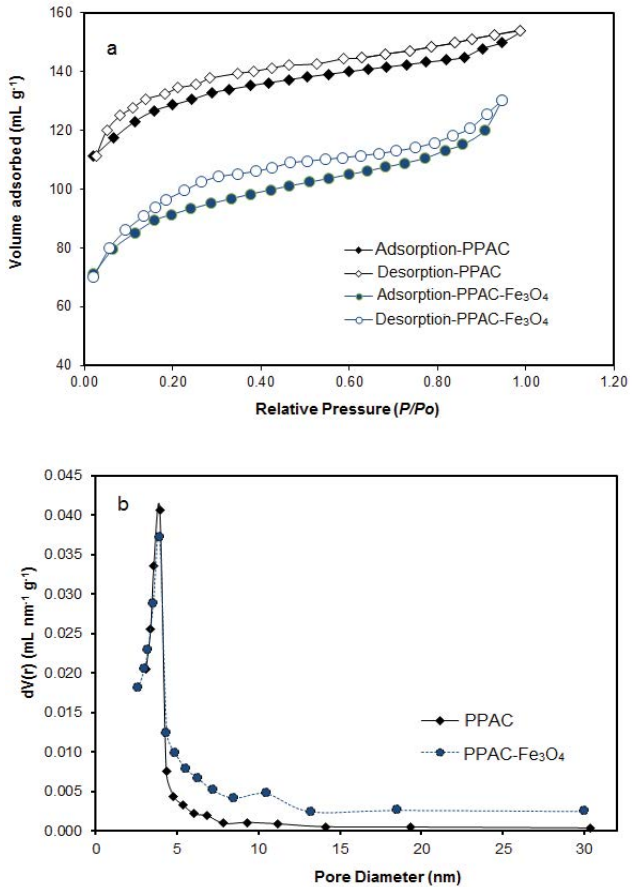

Fig. 2. (a) Nitrogen adsorption–desorption isotherms and (b) pore size distribution of PPAC and PPAC-Fe_3O_4.

process. The type IV adsorption isotherm pattern occurs in the higher P/P_0 area with hysteresis loop of type H1 showing mesoporous material. The volume of adsorbates in all isotherms increases relatively sharply with respect to P/P_0 around 0.6 which indicates nitrogen capillary condensation in regular mesopore structures. The pore size distribution of PPAC and PPAC-Fe_3O_4 derived from the adsorption branch of isotherm shows that the most probable pore size is centered at 3.94 nm (Fig. 2b). The BET surface area of PPAC and PPAC-Fe_3O_4 was 415.12 and 300.09 $m^2 g^{-1}$. The total of pore volume for PPAC and PPAC-Fe_3O_4 was 0.23 and 0.20 $cm^3 g^{-1}$, respectively, while the average pore diameters were 2.69 and 2.21 nm. The average pore diameters of all the samples were in the range of 2 – 10 nm, which belong to mesopores [45,46].

When compared with BET surface area, total pore volume, and average pore diameters between PPAC and PPAC-Fe_3O_4, it shows that the PPAC structure does not change with the presence of Fe_3O_4 particles which support that the PPAC-Fe_3O_4 material is still dominated by PPAC. However, the coating of Fe_3O_4 particles on the PPAC causes a decrease in surface area and pore volume in the PPAC-Fe_3O_4.

From Fig. 3, it can be observed differences in surface morphology between the carbon from the palm shells before activated, PPAC and PPAC-Fe_3O_4 material at 3,000x magnification. At Fig. 3 it can be seen that the PPAC morphology (Fig. 3b) has more cavities than the carbon from the oil palm shells that has not been activated (Fig. 3a), this is also supported by the elemental composition data contained in the EDX spectra which shows an increase % C of carbon before activation from 84.81% (Fig. 3d) to 96.31% (Fig. 3e) in PPAC. In the PPAC, there are uniform pores (Fig. 3b) and after coating Fe_3O_4 particles, there is a decrease in the number of pores in PPAC-Fe_3O_4 (Fig. 3c). The coating of Fe_3O_4 particles on PPAC can also be observed from the surface morphology of PPAC-Fe_3O_4 which shows the presence of Fe_3O_4 particles with a size of about 976.8 nm which is evenly distributed on PPAC (Fig. 3c). Pore reduction in PPAC-Fe_3O_4 is due to significant pore blocking by coating particles of Fe_3O_4) [36]. This is supported by data contained in the results of analysis with EDX which shows that in PPAC-Fe_3O_4 material, besides the presence of C and O elements which are constituent elements of PPAC material (Fig. 3e), there are also Fe elements derived from Fe_3O_4 particles (Fig. 3f).

3.2. Effect of experimental conditions

3.2.1. Effect of pH on the dye adsorption

The effect of pH of the solution is one of the factors that play a role in determining the success of the adsorption process. The effect of pH determines the load on the surface of the adsorbent as an active site [15] and changes in the structure of dyes as adsorbates [45,47]. The effect of pH on the adsorption process of CV dye with PPAC and PPAC-Fe_3O_4 adsorbent was studied by varying the CV dye solutions in the pH range 3–12 (Fig. 4). The surface charge assessed by point of zero charge (pH_{pzc}) is defined as the point where the zeta potential is zero. When pH < $pH_{pzc,}$ the surface charge is positive, and when pH > pH_{pzc}, the surface charge is negative. In this case, the pH_{pzc} of the PPAC and PPAC-Fe_3O_4 determined by the solid addition method are about 6.02 and 7.69, respectively (Table 1).

From Fig. 4 it can be seen that the pH of the solution greatly influences the adsorption process. The percentage of CV dye adsorbed on PPAC and PPAC-Fe_3O_4 continued to increase with increasing pH of the solution and optimum at pH of 10. At low pH (<7), the adsorption process is not optimal because at this pH there is competition between CV molecules and H^+ ions found on the active site of the adsorbent. In an alkaline state (pH 7–10), the H^+ ion decreases so that the CV dye adsorption process is more optimal in alkaline conditions. In contrast, the surface of the PPAC-Fe_3O_4 may get negatively charged at a solution pH higher than $pH_{pzc.}$ Increased pH increases the electrostatic interaction between cationic CV dyes and the negatively charged surface active sites of PPAC and PPAC-Fe_3O_4 [48–50]. Identical results were also informed for the adsorption of CV dye by modified rice straw [51] and adsorbent of AC (*Typha latifolia*)-chitosan composite [52]. The CV dye is a basic dye and has a pKa value of 0.8. Because of this low pKa value, it is ionised for entire experimental pH values and found as a cationic species [52]. At pH > 10, CV dye adsorption on both adsorbents begins to decline, this is due to the formation of hydroxide species which tend to cause precipitation [15].

The percentage of CV dye adsorbed in PPAC-Fe_3O_4 is greater than PPAC, this is due to the increase of active sites

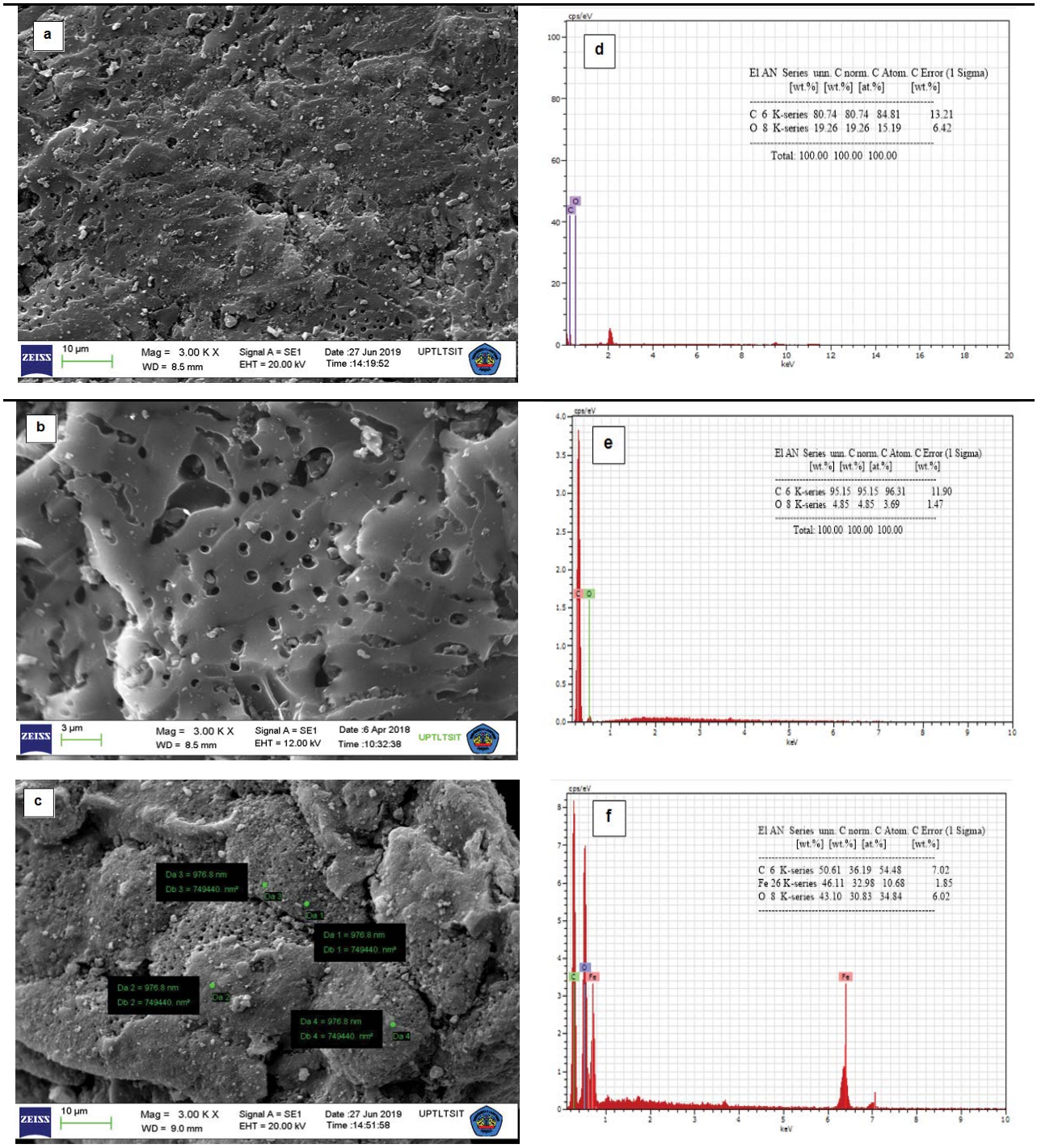

Fig. 3. SEM images and EDX spectra of carbon derived from palm oil shells before activation (a,c), PPAC (b,d), and PPAC-Fe_3O_4 (c,f).

and the magnetic properties of the adsorbent caused by the presence of Fe_3O_4 particles [40,53].

3.2.2. *Effect of adsorbent amount on dye adsorption*

The effect of adsorbent dose is one of the important factors studied to optimize the adsorption process, because the mass of the adsorbent is one of the determining factors in the adsorption process [53]. Increasing the concentration of the adsorbent used will increase the number of active sites of the adsorbent to adsorb the adsorbate. In this study, the effect of the adsorbent dose was carried out by interacting with CV dye solutions using an adsorbent dose range of 0.5–2.5 g L^{-1}. In Fig. 5, it can be observed that there is an increase in % removal of CV dye with increasing adsorbent dosage. Removal of CV dye on PPAC and PPAC-Fe_3O_4 at

Table 1
Determination of point of zero charge (pH_{pzc})

Points of reference		PPAC		PPAC-Fe_3O_4	
$pH_{(initial)}$	$pH_{(final)}$	$pH_{(initial)}$	$pH_{(final)}$	$pH_{(initial)}$	$pH_{(final)}$
0	0				
3	3	3	3.64	3	5.98
4	4	4	4.72	4	7.15
5	5	5	6.53	5	6.65
6	6	6	6.02[a]	6	7.66
7	7	7	5.45	7	7.69[a]
8	8	8	6.43	8	7.02
9	9	9	6.74	9	7.32
10	10	10	7.60	10	7.68

[a]pH_{pzc} for PPAC and PPAC-Fe_3O_4 is 6.02 and 7.69, respectively.

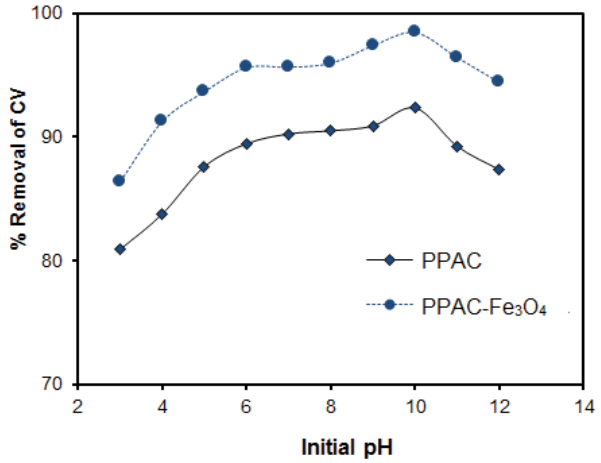

Fig. 4. Influence of pH interaction on adsorption of CV dye onto PPAC and PPAC-Fe_3O_4 (contact time of 60 min, concentration of 10 mg L^{-1}, and temperature of 27°C).

the use of the adsorbent dose of 2.5 g L^{-1} was 90% and 97%, respectively (Fig. 5).

3.2.3. *Effect of contact time on the dye adsorption*

The contact time between the adsorbent and the adsorbate is one of the essential things in the adsorption process because it will have an impact in designing economical procedures in wastewater treatment process [49,54,55]. The contact time between CV dyes with PPAC and PPAC-Fe_3O_4 was studied in the time range of 0–120 min (Fig. 6).

From Fig. 6 it can be observed that the adsorption of CV dyes in both PPAC and PPAC-Fe_3O_4 is relatively fast. In the first 15 min, the adsorption increased sharply with the percentage of CV dye adsorbed on PPAC and PPAC-Fe_3O_4, each at 71.37% and 83.05%. The increase in CV dye adsorption occurred slowly with increasing contact time and reached constant at 90 min interaction time with the percentage of adsorbed CV dye for PPAC and PPAC-Fe_3O_4, respectively, at 86.41% and 95.76%. Furthermore, after 90 min of contact time, the addition of time did not give an increase in the number of adsorbed CV dyes. Thus, it can be stated that at this stage the adsorption process is estimated to have reached equilibrium [15,49].

3.2.4. *Effect of initial dye concentration*

The effect of the initial concentration of CV dye on the adsorption ability of PPAC and PPAC-Fe_3O_4 was studied through the interaction of CV dye solutions at initial concentrations that varied with a range of 0–300 mg L^{-1}. The number of CV dye adsorbed per gram (q_{exp}) vs. the initial concentration in solution (C_0) is shown in Fig. 7. From the figure, it can be observed that there is an increase in the number of CV dye adsorbed with increasing concentrations of CV dye used. The adsorption of CV dye increases sharply at low initial concentrations and gradually increases at high concentrations. This shows that PPAC-Fe_3O_4 has a high adsorption affinity for the CV dye. The increase in

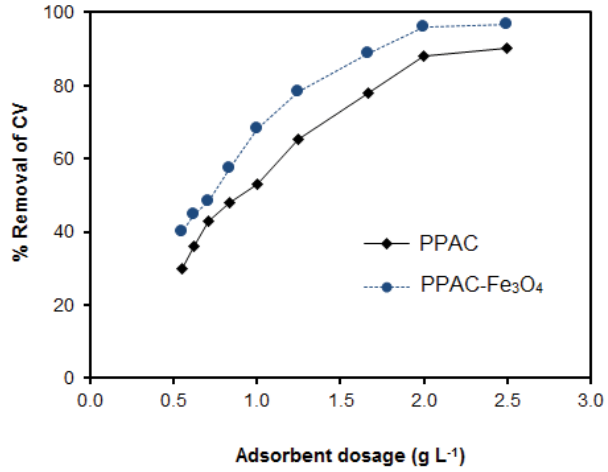

Fig. 5. Influence of adsorbent dose on CV dye removal yield (pH of 10, CV dye concentration of 10 mg L^{-1}, contact time of 60 min, and temperature of 27 °C).

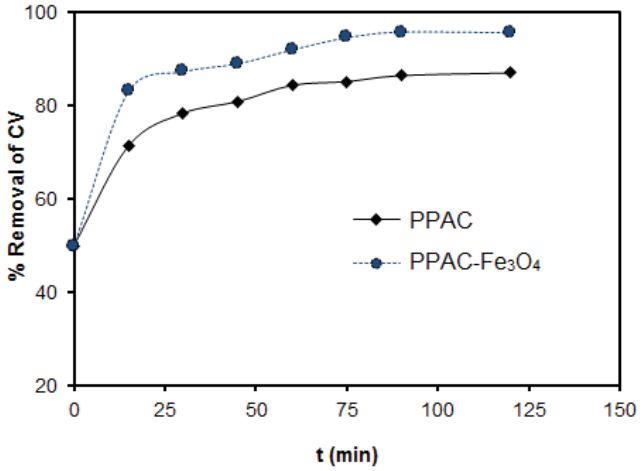

Fig. 6. Influence of contact time on adsorption of CV dye onto PPAC and PPAC-Fe_3O_4 (pH of 10, CV dye concentration of 10 mg L^{-1}, and temperature of 27°C).

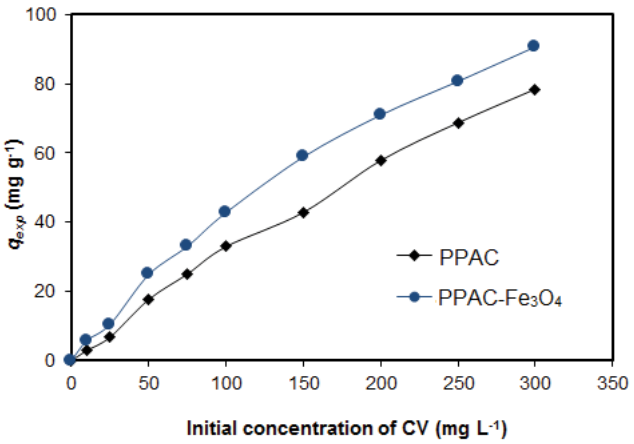

Fig. 7. Influence of initial concentration on adsorption of CV dye onto PPAC and PPAC-Fe_3O_4 (pH of 10, contact time of 90 min, and temperature of 27 C).

adsorption is related to the number of active sites available on the surface of the adsorbent [53].

The adsorption ability of PPAC-Fe_3O_4 material to absorb CV dye solution can also be seen from the UV-Vis spectra of CV dye solutions before and after adsorption using the PPAC-Fe_3O_4 adsorbent (Fig. 8). From Fig. 8 it can be seen that the use of 10 mg L^{-1} CV dye solution produced an absorbance of 1.414 and after adsorption with PPAC-Fe_3O_4 at the adsorbent dose, pH and optimum contact time obtained an absorbance value of 0.012, a decrease in absorbance of around 99.15%. This shows that after the adsorption process by PPAC-Fe_3O_4 there was a decrease in CV dye concentration in solution.

3.3. Adsorption kinetics and isotherm

3.3.1. Kinetic model of CV dye adsorption on PPAC and PPAC-Fe_3O_4

In this study, the CV dye adsorption kinetics model on PPAC and PPAC-Fe_3O_4 was studied by applying pseudo-first-order (Eq. (3)) and pseudo-second-order (Eq. (4)) kinetics model as follows: [56–58]

$$\ln\left(q_e - q_t\right) = \ln\left(q_e\right) k_1 t \tag{3}$$

$$\frac{t}{q_t} = \frac{1}{k_2 q_e^2} + \frac{t}{q_e} \tag{4}$$

where q_t and q_e (mg/g) are total CV dye adsorption capacity at time t and at equilibrium, respectively, k_1 and k_2 are the first order and second order rate constants, respectively. The kinetic data, adsorption rate constant, and regression coefficients of CV dyes on PPAC and PPAC-Fe_3O_4 are presented in Table 2.

The values of q_e and k_1 were determined from the slope and intercept values of the plot between $ln\ (q_e–q_t)$ vs. t as shown in Fig. 9a obtained from the completion of Eq. (5) and the results are summarized in Table 2. Determination of the pseudo-second-order kinetics model was investigated by applying Eq. (6) through plot t/q_t vs. t which produces a slope and intercept to obtain the values of q_e and k_1 as shown in Fig. 9b and Table 2.

The correlation coefficient (R^2) for the pseudo-second-order model for PPAC and PPAC-Fe_3O_4 (R^2 = 0.983 and 0.990) is greater than the pseudo-first-order model (R^2 = 0.818 and 0.861). This shows that the CV dye adsorption kinetics model on PPAC and PPAC-Fe_3O_4 tends to follow the pseudo-second-order kinetics model. The adsorption kinetics model on CV dye in this study is in line with the results of previous studies [49,53,59]. From Table 2 it can be seen that the adsorption rate (k_2) of CV dye by PPAC-Fe_3O_4 is greater than that of PPAC. In PPAC-Fe_3O_4, besides there is a pore on carbon, there are also magnetic properties of adsorbents from Fe_3O_4 particles [15,60].

To find out the mechanism of CV dye adsorption on PPAC and PPAC-Fe_3O_4, the data analysis was carried out using an intraparticle diffusion model proposed by Weber and Morris [45,49].

$$q_t = k_{id} t^{0.5} + C \tag{5}$$

where k_{id} (mg g^{-1} min$^{-0.5}$) is the intraparticle diffusion rate constant, and C value (mg g^{-1}) represents a constant depicting resistance to mass transfer in the boundary layer. The k_{id}

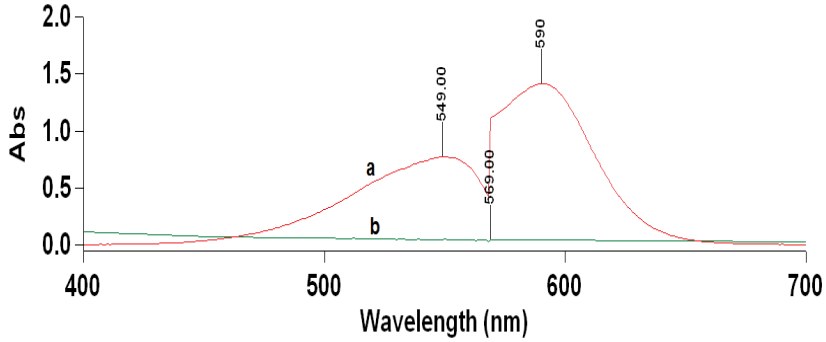

Fig. 8. UV-VIS spectrum of CV dye solution (a) before and (b) after adsorption by PPAC-Fe_3O_4 (adsorbent dose of 2.5 g L^{-1}, pH of 10, CV dye concentration of 10 mg L^{-1}, contact time of 90 min, and temperature of 27°C).

Table 2
Kinetic parameters for the adsorption of CV onto the PPAC and PPAC-Fe_3O_4 at temperature of °C and pH of 10

Adsorbents	$q_{e(exp)}$ (mg g^{-1})	Pseudo-first-order			Pseudo-second-order		
		$q_{e(cal)}$ (mg g^{-1})	k_1 (min^{-1})	R^2	$q_{e(cal)}$ (mg g^{-1})	k_2 (g mg^{-1} min^{-1})	R^2
PPAC	6.960	9.309	0.107	0.818	7. 001	0.059	0.983
PPAC-Fe_3O_4	7.649	11.857	0.139	0.861	8.524	0.088	0.990

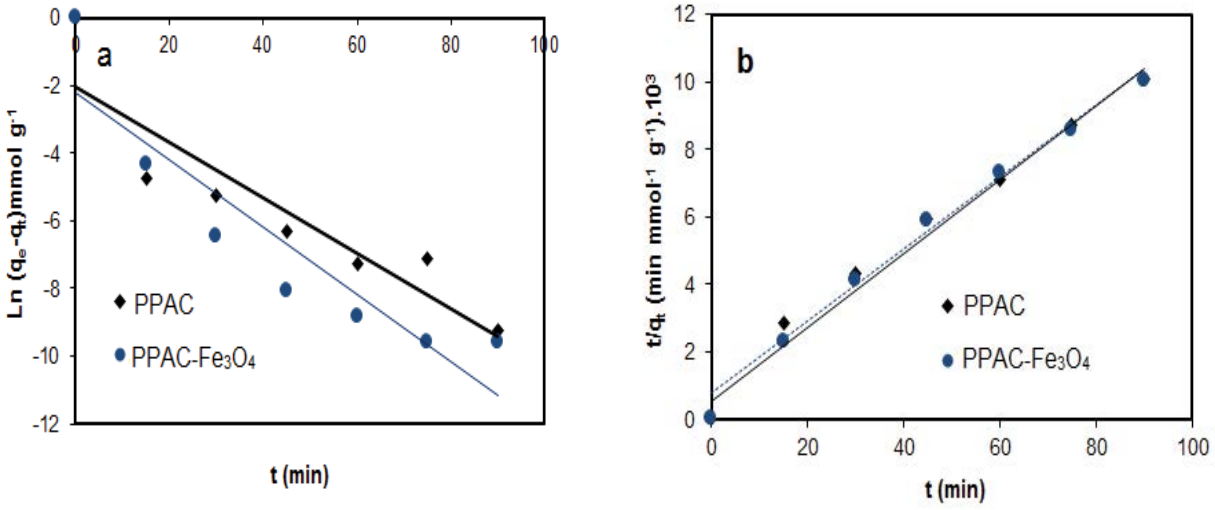

Fig. 9. (a) Pseudo-first-order and (b) pseudo-second-order for adsorption of CV dye on PPAC and PPAC-Fe_3O_4.

and C were calculated from the slope and intercept of lines obtained from plots of q_t vs. $t^{0.5}$. Value of k_{id} and C were evaluated from the slope and intercepts in Fig. 10 and the value of k_{id} and C is displayed in Table 3.

If the intraparticle diffusion obtained from the results of a plot of q_t vs. $t^{0.5}$ is a linear and passes through the origin then the intraparticle diffusion rate is not the diffusion control film [61]. In Fig. 10 it can be seen that all the plots have two linear parts. This feature shows that more than one mode of adsorption is involved. The first linear part accommodates the adsorption phase of 0–60 min, which indicates external mass transfer. The second linear part accommodates the adsorption phase of 60–120 min, indicating intraparticle diffusion. The second linear parts do not cross the origin (C≠0), recommending that intraparticle diffusion is not the only rate controlling step and the external mass transfer is also happening synchronously [45]. A similar intraparticle diffusion result was obtained for the adsorption of diquat herbicide onto magnetic carbon nanotubes [62].

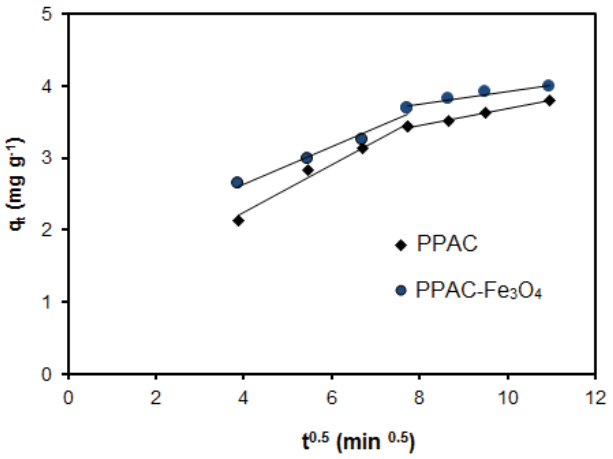

Fig. 10. Intraparticle difussion plot for CV dye adsorbed onto PACC and PPAC-Fe_3O_4.

3.3.2. Adsorption isotherms

The adsorption isotherm patterns of CV dye on PPAC and PPAC-Fe_3O_4 were investigated using the adsorption isotherm models of Langmuir (Eq. (6)), Freundlich (Eq. (7)), and Dubinin–Radushkevich (DR) (Eq. (8)) [63,64]. The adsorption isotherm models of CV dye on PPAC and PPAC-Fe_3O_4 are shown in Fig. 11. The adsorption data were analyzed using the adsorption isotherm equation to produce the characteristics of the adsorption parameters presented in Table 4.

The Langmuir adsorption isotherm model assumes that on the surface of the adsorbent there are a certain number of active sites that are proportional to the surface area, the surface of the adsorbent is uniform and the adsorption process is monolayer expressed in Eq. (6) [65,66].

$$\frac{1}{q_e} = \frac{1}{q_m K_L C_e} + \frac{1}{q_m} \quad (6)$$

Table 3
Intraparticle diffussion model for CV dye adsorption onto PPAC and PPAC-Fe_3O_4

Adsorbent	Initial linear portion			Second linear portion		
	k_{i1} (mg g^{-1} min$^{-0.5}$)	C_1 (mg g^{-1})	R_1^2	k_{i2} (mg g^{-1} min$^{-0.5}$)	C_2 (mg g^{-1})	R_2^2
PPAC	0.329	0.922	0.982	0.117	2.514	0.994
PPAC-Fe_3O_4	0.259	1.596	0.968	0.092	3.040	0.926

where C_e (mg L^{-1}) is the equilibrium concentration of CV dye solution, q_e (mg g^{-1}) is the CV dye adsorption capacity at equilibrium, q_m is the monolayer adsorption capacity, and K_L is the equilibrium constants including the affinity of binding sites (L mg^{-1}). K_L and q_m can be determined from the linear equation of plot log $1/q_e$ vs. C_e which produce a straight line with $1/q_m K_L$ as the slope and $1/q_m$ as intercept.

In addition, the Freundlich adsorption isotherm model is an empirical equation employed for heterogeneous system and adsorption at multilayers [67] represented by Eq. (7).

$$\log q_e = \log K_F + \frac{1}{n}\log C_e \tag{7}$$

where K_F ((mg g^{-1}) (L mg^{-1})$^{1/n}$) is the adsorption capacity factor and n is the adsorption intensity factor with n values ranging from 1 to 10 [68]. Next, the plot of log q_e vs. log C_e produces K_F and exponent n.

The D-R adsorption isotherm can be used to explain the adsorption that occurs on a homogeneous and heterogeneous surface. The D-R adsorption isotherm model can be expressed as Eq. (8).

$$\ln q_e = q_{DR} - 2B_{DR}RT\ln\left(\frac{1+1}{C_e}\right) \tag{8}$$

where R is the gas constant (8.314 kJ mol^{-1}), and T is the absolute temperature (K), q_{DR} and B_{DR} are the D-R isotherm constants in mg g^{-1} and mol^2 kJ^{-2}, respectively. Plot log q_e vs. ln $(1 + 1/C_e)$ produces slope and intercept.

The CV dye adsorption parameters by PPAC and PPAC-Fe_3O_4 contained in Table 4 show the regression coefficients of linear equations (R) of Freundlich adsorption isotherm models (PPAC and PPAC-Fe_3O_4 0.992 and 0.991, respectively) greater than the D-R and Langmuir adsorption isotherms. This shows that the CV dye adsorption isotherm is more in line with the Freundlich adsorption isotherm model which is supported by the adsorption pattern from the experimental results closer to the Freundlich model (Fig. 11). The Freundlich adsorption isotherm states that the CV dying adsorption process occurs on material surfaces with heterogeneous multilayers. This indicates that the CV dye adsorption on PPAC and PPAC-Fe_3O_4 is dominated by physical interactions that occur through the pores of active carbon. While the magnetic properties of the adsorbent in PPAC-Fe_3O_4 can also increase the number of adsorbed CV dye [69]. In Table 4 it can be observed that the number of adsorbed CV dye determined from the experimental results ($q_{m(exp)}$) on PPAC and PPAC-Fe_3O_4 was 88.495 and 95.715 mg g^{-1}, respectively. In literature, it was reported that the adsorption isotherms of various organic compounds onto activated carbon followed the Freundlich isotherm model [70,71].

The adsorption capacity ($q_{m(exp)}$) results of this study can be compared with some carbon-based CV dye adsorbents (Table 5). From the comparison results, it can be observed that the PPAC-Fe_3O_4 adsorbent is one of the good adsorbents to absorb the CV dye in solution, especially in the waste treatment process containing the CV dye.

3.4. Reusability of adsorbent

One important consideration in the use of adsorbents is the ability to reuse or regenerate, because it is a factor that determines economic visibility and cost effectiveness in the sustainability of its use in reducing environmental pollution. In the experiment, the ability to reuse PPAC-Fe_3O_4 adsorbent in adsorbing CV dye was determined by doing the adsorption–desorption process for five repetitions (Fig. 12). The results of the adsorption of CV dye solution released (desorption) with 0.05 M HCl solution repeatedly four times did not reduce the amount of adsorbed CV dye and produced 80% adsorbed CV dye (Fig. 12). Material reusability of adsorbate adsorption for some cycles without breakage of material structure and alleviating capacity

Table 4
Langmuir, Freundlich, and D-R parameters for the adsorption of CV dye on PPAC and PPAC-Fe_3O_4 at temperature of 27°C, pH of 10, and contact time of 90 min

	Adsorbent	PPAC	PPAC-Fe_3O_4
	$q_{m(exp)}$ (mg g^{-1})	88.495	95.715
Model			
Langmuir			
	q_m (mg g^{-1})	81.301	84.746
	$K_L \times 10^{-2}$ (L mol^{-1})	1.454	2.106
	R^2	0.539	0.664
Freundlich			
	K_F (mg g^{-1}) (L mg^{-1})$^{1/n}$	1.066	2.852
	n	0.985	1.210
	R^2	0.992	0.991
Dubinin–Radushkevich (D-R)			
	q_{DR} (mg g^{-1})	96.188	119.677
	B_{DR}	2.6×10^{-6}	2.7×10^{-7}
	R^2	0.934	0.963

of adsorption is one of the key factors in controlling the material quality generated [75].

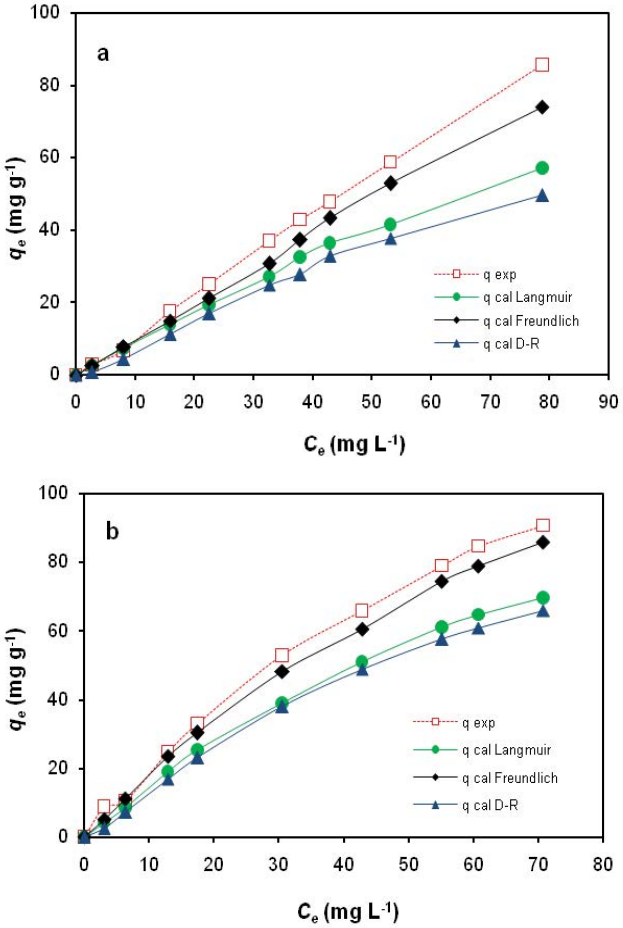

Fig. 11. Adsorption isotherm of CV dye on (a) PPAC and (b) PPAC-Fe_3O_4 based on experiment (q_{exp}) and estimation (q_{cal}) results using adsorption isotherm equations.

4. Conclusions

Coating of Fe_3O_4 particles on PPAC to produce magnetic carbon-based adsorbents has increased the carbon adsorption ability to crystal violet (CV) dye. Using this technique, the obtained PPAC-Fe_3O_4, which has a large adsorption rate and capacity for CV dyes in solution, can separate target compounds quickly and effectively, as well as does not cause side products that are harmful to the environment. Adsorption of CV dyes on PPAC and PPAC-Fe_3O_4 was optimum at pH 10 with an adsorbent dose of 2.5 g L^{-1}, and contact time of 90 min. The CV dye adsorption kinetics model on PPAC and PPAC-Fe_3O_4 tends to follow the pseudo-second-order kinetic model with the rate constants (k_2) for PPAC and PPAC-Fe_3O_4 of 0.059 and 0.088 (g mg^{-1} min^{-1}), respectively. In addition, the adsorption isotherm model of CV dyes on PPAC and PPAC-Fe_3O_4 tends to follow the Freundlich adsorption isotherm with K_F values of 1.066 and 2.852 (mg g^{-1}) (L mg^{-1})$^{1/n}$, respectively. The tendency of CV dye adsorption models follows the model of Freundlich adsorption isotherm which illustrates that CV dye adsorption processes occur on

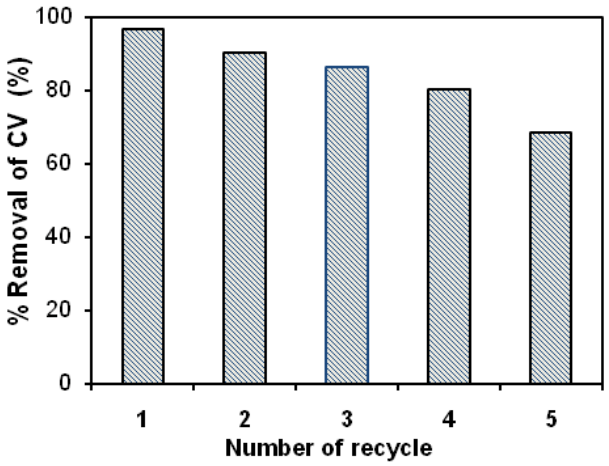

Fig. 12. Variation of the CV dye adsorption capacity of regenerated PPAC-Fe_3O_4 as function of regeneration cycles.

Table 5
Adsorption capacity of CV dye on PPAC-Fe_3O_4 compared with other activated carbon-based adsorbents

Adsorbent	q_m (mg g^{-1})	Experimental condition (pH and temperature)	References
AC (*Typha latifolia*)-chitosan composite	0.27	9.0 and 30°C	[52]
Rice husk activated carbon	11.18	10.8 and 25°C	[72]
AC (Common Reed)	38.50	7.0 and 30°C	[73]
AC (Waste apricot)	52.86	– and 30°C	[74]
Phosphoric acid activated carbon (PAAC)	60.42	6.0 and 25°C	[7]
Magnetically modified activated carbon	67.10	9.0 and 50°C	[69]
Magnetic carbon-iron oxide nanocomposite	81.70	8.5 and 50°C	[60]
AC-AgNPLs (Ag nanoparticles (AgNPLs) chemically immobilized onto activated carbon)	87.20	7.5 and 30°C	[49]
PPAC-Fe_3O_4	95.71	10.0 and 27°C	This work

heterogeneous surfaces with multilayers. This indicates that CV dye adsorption on PPAC-Fe_3O_4 is dominated by physical interactions that occur through the pores of activated carbon and the magnetic properties of the adsorbent on PPAC-Fe_3O_4 have increased the number of adsorbed CV dyes. Adsorbate is relatively easier to release, so the adsorbent can be used repeatedly. Thus the activated carbon from oil palm shells has economic value and can be used as an adsorbent in the treatment of toxic chemical waste to reduce environmental pollution.

Acknowledgements

The authors thank the Directorate of Research and Community Service, Directorate General for Research and Development, Ministry of Research, Technology and Higher Education of the Republic of Indonesia for funding this research in accordance with contract number: 065/SP2H/LT/DPRM/2019 and international seminar funds in 2019. The authors give a high appreciation to Technical Service Unit of the Integrated Laboratory and the Technology Innovation Center–University of Lampung (UPT Laboratorium Terpadu dan Sentra Inovasi Teknologi–Universitas Lampung).

References

[1] V. Ramya, D. Murugan, C. Lajapathirai, P. Saravanan, A. Sivasamy, Removal of toxic pollutants using tannery sludge derived mesoporous activated carbon: experimental and modelling studies, J. Environ. Chem. Eng., 7 (2019) 1–13.
[2] Suharso, Buhani, Biosorption of Pb(II), Cu(II) and Cd(II) from aqueous solution using cassava peel waste biomass, Asian J. Chem., 23 (2011) 1112–1116.
[3] N.L. Nemerrow, Liquid Waste of Industry, Addison Wesley Publishing Company, California, 1971.
[4] S.A. Snyder, Emerging chemical contaminants: Looking for better harmony, J. AWWA, 106 (2014) 38–52.
[5] M.S. Tsuboy, J.P. Angeli, M.S. Mantovani, S. Knasmüller, G.A. Umbuzeiro, L.R. Ribeiro, Gentoxic, mutagenic and cytotoxic effects of the commercial dye CI disperse blue 291 in the human hepatic cell line HepG2. Toxicol. in Vitro, 21 (2007) 1650–1655.
[6] S. Vinitnantharat, W. Chartthe, A. Pinisakul, Toxicity of reactive dye 141 and basic red 14 to algae and water fleas, Water Sci. Technol., 58 (2008) 1193–1198.
[7] S. Senthilkumaar, P. Kalaamani, C.V. Subburaam, Liquid phase adsorption of crystal violet onto activated carbons derived from male flowers of coconut tree, J. Hazard. Mater., B136 (2006) 800–808.
[8] S. Kaur, S. Rani, R.K. Mahajan, Adsorptive removal of dye crystal violet onto low-cost carbon produced from *Eichhornia* plant: kinetic, equilibrium, and thermodynamic studies, Desal. Wat. Treat., 53 (2015) 543–556.
[9] M. Sharma, K. Anubha, C.P. Kaushik, Waste biomass of *Nostoc linckia* as adsorbent of crystal violet dye: Optimization based on statistical model, Int. Biodeterior. Biodegrad., 65 (2011) 513–521.
[10] C.S. Umpierres, L.D.T. Prola, M.A. Adebayo, E.C. Lima, G.S. dos Reis, D.D.F. Kunzler, G.L. Dotto, L.T. Arenas, E.V. Benvenutti, Mesoporous Nb_2O_5/SiO_2 material obtained by sol–gel method and applied as adsorbent of crystal violet dye, Environ. Technol., 38 (2017) 566–578.
[11] V. Vaiano, O. Sacco, D. Sannino, P. Ciambelli, Nanostructured N-doped TiO_2 coated on glass spheres for the photocatalytic removal of organic dyes under UV or visible light irradiation, Appl. Catal. B Environ., 170–171 (2015) 153–161.
[12] G.C. Collazzo, D.S. Paz, S.L. Jahn, N.L.V. Carreño, E.L. Foletto, Evaluation of niobium oxide doped with metals in photocatalytic degradation of leather dye, Latin Am. Appl. Res., 42 (2012) 51–54.
[13] T. Saitoh, M. Saitoh, C. Hattori, M. Hiraide, Rapid removal of cationic dyes from water by co precipitation with aluminum hydroxide and sodium dodecyl sulfate, J. Environ. Chem. Eng., 2 (2014) 752–758.
[14] K. Saeed, M. Ishaq, S. Sultan, I. Ahmad, Removal of methyl violet 2-B from aqueous solutions using untreated and magnetite-impregnated almond shell as adsorbents, Desal. Wat. Treat., 57 (2016) 13484–13493.
[15] Buhani, F. Hariyanti, Suharso, Rinawati, Sumadi, Magnetized algae-silica hybrid from *Porphyridium* sp. biomass with Fe_3O_4 particle and its application as adsorbent for the removal of methylene blue from aqueous solution, Desal. Wat. Treat., 142 (2019) 331–340.
[16] J.S. Wu, C.H. Liu, K.H. Chu, S.Y. Suen, Removal of cationic dye methyl violet 2B from water by cation exchange membranes, J. Membr. Sci., 309 (2008) 239–245.
[17] C.S.D. Rodrigues, L.M. Madeira, R.A.R. Boaventura, Synthetic textile dyeing wastewater treatment by integration of advanced oxidation and biological processes performance analysis with costs reduction, J. Environ. Chem. Eng., 2 (2014) 1027–1039.
[18] T. Pankaj, P.A. Joy, Superparamagnetic nanocomposite of magnetite and activated carbon for removal of dyes from waste water, Nanosci. Nanotechnol. Lett., 1 (2009) 171–175.
[19] I. Ali, M. Asim, T.A. Khan, Low-cost adsorbents for the removal of organic pollutants from wastewater, J. Environ. Manage., 113 (2012) 170–183.
[20] Buhani, Narsito, Nuryono, E.S. Kunarti, Suharso, Adsorption competition of Cu(II) ion in ionic pair and multi-metal solution by ionic imprinted amino-silica hybrid adsorbent, Desal. Wat. Treat., 55 (2015) 1240–1252.
[21] H. Chaudhuri, S. Dash, S. Ghorai, S. Pal, A. Sarkar, SBA-16: Application for the removal of neutral, cationic, and anionic dyes from aqueous medium, J. Environ. Chem. Eng., 4 (2016) 157–166.
[22] T. Calvete, E.C. Lima, N.F. Cardoso, S.L.P. Dias, E.S. Ribeiro, Removal of brilliant green dye from aqueous solutions using home made activated carbons, Clean Air Soil Water., 38 (2010) 521–532.
[23] E. Ayranci, O. Duman, In-situ UV-visible spectroscopic study on the adsorption of some dyes onto activated carbon cloth, Sep. Sci. Technol., 44 (2009) 3735–3752.
[24] O. Duman, S. Tunç, T.G. Polat, Adsorptive removal of triarylmethane dye (Basic Red 9) from aqueous solution by sepiolite as effective and low-cost adsorbent, Microporous Mesoporous Mater., 210 (2015) 176–184.
[25] O. Duman, S. Tunç, T.G. Polat, Determination of adsorptive properties of expanded vermiculite for the removal of C. I. Basic Red 9 from aqueous solution: kinetic, isotherm and thermodynamic studies, Appl. Clay Sci., 109–110 (2015) 22–32.
[26] O. Duman, S. Tunç, B.K. Bozoğlan, T.G. Polat, Removal of triphenylmethane and reactive azo dyes from aqueous solution by magnetic carbon nanotube-κ-carrageenan-Fe_3O_4 nanocomposite, J. Alloys Comp., 687 (2016) 370–383.
[27] Q. Li, Y. Qi, C. Gao, Chemical regeneration of spent powdered activated carbon used in decolorization of sodium salicylate for the pharmaceutical industry, J. Clean. Prod., 86 (2015) 424–431.
[28] N. Singh, C. Balomajumder, Simultaneous removal of phenol and cyanide from aqueous solution by adsorption onto surface modified activated carbon prepared from coconut shell, J. Water Process. Eng., 9 (2016) 233–245.
[29] Z. Gong, S. Li, J. Ma, X. Zhang, Synthesis of recyclable powdered activated carbon with temperature responsive polymer for bisphenol a removal, Sep. Purif. Technol., 157 (2016) 131–140.
[30] Y.L. Kang, S.T. Khoon, P. Monash, S. Ibrahim, P. Saravanan, Adsorption isotherm, kinetic and thermodynamic studies of activated carbon prepared from *Garcinia mangostana* shell, Asia-Pacific J. Chem. Eng., 8 (2013) 811–818.
[31] N. Ozbay, A.S. Yargic, Factorial experimental design for Remazol Yellow dye sorption using apple pulp/apple pulp carbon–titanium dioxide co-sorbent, J. Clean. Prod., 100 (2015) 333–343.
[32] H. Sayğılı, F. Güzel, Y. Önal, Conversion of grape industrial processing waste to activated carbon sorbent and its

performance in cationic and anionic dyes adsorption, J. Clean. Prod., 93 (2015) 84–93.
[33] O. Duman, S. Tunç, T.G. Polat, B.K. Bozoğlan, Synthesis of magnetic oxidized multiwalled carbon nanotube-κ-carrageenan-Fe_3O_4 nanocomposite adsorbent and its application in cationic methylene blue dye adsorption, Carbohydr. Polym., 147 (2016) 79–88.
[34] S.H. Araghi, M.H. Entezari, Amino-functionalized silica magnetite nanoparticles for the simultaneous removal of pollutants from aqueous solution, *Appl. Surf. Sci.*, 333 (2015) 68–77.
[35] M. Ishaq, S. Sultan, I. Ahmad, H. Ullah, M. Yaseen, A. Amir, Adsorptive desulfurization of model oil using untreated, acid activated and magnetite nanoparticle loaded bentonite as adsorbent, J Saudi Chem. Soc., 21 (2017) 143–151.
[36] K.T. Wong, Y. Yoon, S.A. Snyder, M. Jang, Phenyl-functionalized magnetic palm-based powdered activated carbon for the effective removal of selected pharmaceutical and endocrine-disruptive compounds, Chemosphere, 152 (2016) 71–80.
[37] T.S. Anirudhan, F. Shainy, Adsorption behaviour of 2-mercaptobenzamide modified itaconic acid-grafted-magnetite nanocellulose composite for cadmium(II) from aqueous solutions, J. Ind. Eng. Chem., 32 (2015) 157–166.
[38] I. Mohmood, C.B. Lopes, I. Lopes, D.S. Tavares, A.M. Soares, A.C. Duarte, T. Trindade, I. Ahmad, E. Pereira, Remediation of mercury contaminated saltwater with functionalized silica coated magnetite nanoparticles, Sci. Total Environ., 557–558 (2016) 712–721.
[39] Q. Zhang, T. Lu, D.M. Bai, D.Q. Lin, S.J. Yao, Self-immobilization of a magnetic biosorbent and magnetic induction heated dye adsorption processes, Chem. Eng. J., 284 (2016) 972–979.
[40] Buhani, Rinawati, Suharso, D.P. Yuliasari, S.D. Yuwono, Removal of Ni(II), Cu(II), and Zn(II) ions from aqueous solution using *Tetraselmis* sp. biomass modified with silica-coated magnetite nanoparticle, Desal. Wat. Treat., 80 (2017) 203–213.
[41] L. Qimeng, Q. Yanshan, G. Canzhu, Chemical regeneration of spent powdered activated carbon used in decolorization of sodium salicylate for the pharmaceutical industry, J. Clean. Prod., 86 (2015) 424–431.
[42] Buhani, M. Puspitarini, Rahmawaty, Suharso, M. Rilyanti, Sumadi, Adsorption of phenol and methylene blue in solution by oil palm shell activated carbon prepared by chemical activation, Orient. J. Chem., 34 (2018) 2043–2050.
[43] C. Desbrow, E. Routledge, G. Brighty, J. Sumpter, M. Waldock, Identification of estrogenic chemicals in STW effluent. 1. Chemical fractionation and in vitro biological screening, Environ. Sci. Technol., 32 (1998) 1549–1558.
[44] H.P.S. Abdul Khalil, M. Jawaid, P. Firoozian, U. Rashid, A. Islam, H. Akil, Activated carbon from various agricultural wastes by chemical activation with KOH: preparation and characterization, J. Biobased Mater. Bioenergy, 7 (2013) 1–7.
[45] Y.D. Liang, Y.J. He, T.T. Wang, L.H. Lei, Adsorptive removal of gentian violet from aqueous solution using $CoFe_2O_4$/activated carbon magnetic composite, J. Water. Process Eng., 27 (2019) 77–88.
[46] D.W. Cho, J. Lee, Y.S. Ok, E.E. Kwon, H. Song, Fabrication of a novel magnetic carbon nanocomposite adsorbent via pyrolysis of sugar, Chemosphere, 163 (2016) 305–312.
[47] R. Hoppe, G. Alberti, U. Costantino, C. Dionigi, G.N. Schulz-Ekloff, R. Vivani, Intercalation of dyes in layered zirconium phosphates. 1. Preparation and spectroscopic characterization of α-zirconium phosphate crystal violet compounds, Langmuir, 13 (1997) 7252–7257.
[48] S. Chakraborty, S. Chowdury, P.D. Saha, Adsorption of crystal violet from aqueous solution onto NaOH-modified rice husk, Carbohydr. Polym., 86 (2011) 1533–1541.
[49] A.H. AbdEl-Salam, H.A. Ewais, A.S. Basaleh, Silver nanoparticles immobilised on the activated carbon as efficient adsorbent for removal of crystal violet dye from aqueous solutions. A kinetic study, J. Mol. Liq., 248 (2017) 833–841.
[50] P. Sun, C. Hui, R.A. Khan, X. Guo, S. Yang, Y. Zhao, Mechanistic links between magnetic nanoparticles and recovery potential and enhanced capacity for crystal violet of nanoparticles-coated kaolin, J. Clean. Prod., 164 (2017) 695–702.
[51] S. Chowdhury, S. Chakraborty, P. Das, Adsorption of crystal violet from aqueous solution by citric acid modified rice straw: equilibrium, kinetics, and thermodynamics, Sep. Purif. Technol., 48 (2013) 1339–1348.
[52] H.J. Kumari, P. Krishnamoorthy, T.K. Arumugam, S. Radhakrishnan, D. Vasudevan, An efficient removal of crystal violet dye from waste water by adsorption onto TLAC/chitosan composite: a novel low cost adsorbent, Int. J. Biol. Macromol., 96 (2016) 324–333.
[53] N. Atar, A. Olgun, S. Wang, Adsorption of cadmium(II) and zinc(II) on boron enrichment process waste in aqueous solutions: Batch and fixed-bed system studies, Chem. Eng. J., 192 (2012) 1–7.
[54] R. Noroozi, T.J. Al-Musawi, H. Kazemian, M. Zarrabi, Removal of cyanide using surface-modified Linde Type-A zeolite nanoparticles as an efficient and eco-friendly material; J. Water Process Eng., 21 (2018) 44–51.
[55] E. Vaiopoulou, P. Gikas, Effects of chromium on activated sludge and on the performance of wastewater treatment plants, Water Res., 46 (2012) 549–570.
[56] Buhani, Suharso, H. Satria, Hybridization of Nannochloropsis sp. biomass-silica through sol-gel process to adsorb Cd(II) ion in aqueous solutions, Eur. J. Sci. Res., 51 (2011) 467–476.
[57] A.M. Aljeboree, A.F. Alkaim, A.H. Al-Dujaili, Adsorption isotherm, kinetic modeling and thermodynamics of crystal violet dye on coconut husk-based activated carbon, Desal. Wat. Treat., 53 (2015) 3656–3667.
[58] J. Georgin, G.L. Dotto, M.A. Mazutti, E.L. Foletto, Preparation of activated carbon from peanut shell by conventional pyrolysis and microwave irradiation-pyrolysis to remove organic dyes from aqueous solutions, J. Environ. Chem. Eng., 4 (2016) 266–275.
[59] L.L. Embrick, K.M. Porter, A. Pendergrass, D.J. Butcher, Characterization of lead and arsenic contamination at Barber Orchard, Haywood County, NC, Microchem. J., 81 (2005) 117–121.
[60] K.P. Singh, S. Gupta, A.K. Singh, S. Sinha, Optimizing adsorption of crystal violet dye from water by magnetic nanocomposite using response surface modeling approach, J. Hazard. Mater., 186 (2011) 1462–1473.
[61] N.A. Oladoja, A.K. Akinlabi, Congo red biosorption on palm kernel seed coat, Ind. Eng. Chem. Res., 48 (2009) 6188–6196.
[62] O. Duman, C. Özcan, T. Gürkan Polat, S. Tunç, Carbon nanotube-based magnetic and non-magnetic adsorbents for the high-efficiency removal of diquat dibromide herbicide from water: OMWCNT, OMWCNT-Fe_3O_4 and OMWCNT-κ-carrageenan-Fe_3O_4 nanocomposites, Environ. Pollut., 244 (2019) 723–732.
[63] Buhani, Suharso, A.Y. Fitriyani, Comparative study of adsorption ability of Ni(II) and Zn(II) ionic imprinted amino-silica hybrid toward target metal in solution, Asian J. Chem., 25 (2013) 2875–2880.
[64] D. Mitrogiannis, G. Markou, A. Çelekli, H. Bozkurt, Biosorption of methylene blue onto *Arthrospira platensis* biomass: kinetic, equilibrium and thermodynamic studies, J. Environ. Chem. Eng., 3 (2015) 670–680.
[65] X. Xin, Q. Wei, J. Yang, L. Yan, R. Feng, G. Chen, B. Du, H. Li, Highly efficient removal of heavy metal ions by amine-functionalized mesoporous Fe_3O_4 nanoparticles, Chem. Eng. J., 184 (2012) 132–140.
[66] I. Larraza, M. Lŏpez-Gŏnzales, T. Corrales, G. Marcelo. Hybrid materials: magnetite-ployethyenimine-montromolillonite, as magnetic adsorbents for Cr (VI) water treatment, J. Colloid Interface Sci., 385 (2012) 24–33.
[67] Y. Shao, L. Zhou, C. Bao, J. Ma, M. Liu, F. Wang, Magnetic responsive metal–organic frameworks nanosphere with core–shell structure for highly efficient removal of methylene blue, Chem. Eng. J., 283 (2016) 1127–1136.
[68] Y.S. Ho, J.F. Porter, G. McKay, Equilibrium isotherm studies for the sorption of divalent metal ions onto peat: copper, nickel, and lead single component systems, Water Air Soil Pollut., 141 (2002) 1–33.
[69] S. Hamidzadeh, M. Torabbeigi, S.J. Shahtaheri, Removal of crystal violet from water by magnetically modified activated

carbon and nanomagnetic iron oxide, J. Environ. Health Sci. Eng., 13 (2015) 1–7.
[70] E. Ayranci, O. Duman, Removal of anionic surfactants from aqueous solutions by adsorption onto high area activated carbon cloth studied by in situ UV spectroscopy, J. Hazard. Mater., 148 (2007) 75–82.
[71] E. Ayranci, O. Duman, Adsorption of aromatic organic acids onto high area activated carbon cloth in relation to wastewater purification, J. Hazard. Mater., 136 (2006) 542–552.
[72] K. Mohanty, J.T. Naidu, B.C. Meikap, M.N. Biswas, Removal of crystal violet from wastewater by activated carbons prepared from rice husk, Ind. Eng. Chem. Res., 45 (2006) 5165–5171.
[73] M.A. Shouman, W.E. Rashwan, Studies on adsorption of basic dyes on activated carbon derived from *Phragmites australis* (Common Reed), Univers, J. Environ. Res. Technol., 2 (2012) 119–134.
[74] Y. Onal, Kinetics of adsorption of dyes from aqueous solution using activated carbon prepared from waste apricot, J. Hazard. Mater., 137 (2006) 1719–1728.
[75] Buhani, Suharso, L. Aprilia, Chemical stability and adsorption selectivity on Cd^{2+} ionic imprinted *Nannochloropsis* sp. material with silica matrix from tetraethyl orthosilicate, Indo. J. Chem., 12 (2012) 94–99.